DALTON

Syntheses, electrochemistry, photophysics and photochemistry of nitridorhenium(v) diphosphine complexes and related nitridorhenium(v) organometallics; crystal structure of $[Re^{V}N(C{\equiv}CBu^{t})_2(PPh_3)_2]$

Vivian Wing-Wah Yam,* Kwok-Kwong Tam and Kung-Kai Cheung

Department of Chemistry, The University of Hong Kong, Pokfulam Road, Hong Kong

A series of nitrido complexes $[ReNL_2X]^{n+}$ [L = dppe($Ph_2PCH_2CH_2PPh_2$), X = F, Cl, Br, NCS, NCO or N_3 (n = 1) or MeCN (n = 2); L = dppbz($Ph_2PC_6H_4PPh_2$-*o*), X = Cl (n = 1) or MeCN (n = 2)] have been synthesized and shown to exhibit long-lived photoluminescence in both the solid state and fluid solution, derived from the $[(d_{xy})^1(d_{\pi^*})^1]$ triplet (d_{π^*} = d_{xz}, d_{yz}). The positions of the d–d absorption and emission bands have been found to be dependent on the identity of X. The luminescence quantum yields of $[ReNL_2(MeCN)]^{2+}$ are greatly enhanced with respect to their chloro analogues. Cyclic voltammetric studies show that the $[ReNL_2X]^{+}$ complexes display an irreversible reduction couple at E_{pc} of *ca.* −2.0 to −2.3 V and an irreversible oxidation couple at E_{pa} of *ca.* +1.3 to +1.9 V *vs.* the ferrocenium–ferrocene couple in MeCN (0.1 mol dm^{-3} NBu_4PF_6). An additional irreversible reduction couple is observed at *ca.* −1.67 and −1.63 V for $[ReN(dppe)_2(MeCN)]^{2+}$ and $[ReN(dppbz)_2(MeCN)]^{2+}$, respectively. The reactivities of the nitrido complexes toward trifluoroacetic acid and electron donors such as alkoxybenzenes and organic amines have been investigated by Stern–Volmer quenching experiments and transient absorption difference spectroscopy. The electrochemical and spectroscopic properties of $[ReNL_2X]^{n+}$ have been compared with those of organorhenium(v) nitrido complexes $[ReNR_2(PPh_3)_2]$ (R = C≡CBu^t or C_6H_4Me-*p*). The crystal structure of $[ReN(C{\equiv}CBu^{t})_2(PPh_3)_2]$ has been determined: monoclinic, space group $P2_1/n$, a = 13.708(8), b = 19.161(6), c = 17.246(3) Å, β = 109.49(4)°, U = 4270(3) Å^3, Z = 4. A Re≡N distance of 1.63(2) Å has been measured.

Recently, transition-metal–ligand multiply bonded species have attracted considerable attention and have been the subject of numerous studies.[1] Recent work on oxo and nitrido d^2 rhenium(v) complexes by us and others showed that they exhibit interesting and rich photophysical behaviour.[2–4] In an earlier communication,[2b] we reported that the luminescence quantum yield of $[ReN(dppe)_2(MeCN)]^{2+}$ [dppe = 1,2-bis(diphenylphosphino)ethane] is greatly enhanced with respect to its chloro analogue, $[ReN(dppe)_2Cl]^{+}$. In order to have a clearer understanding on the mechanism of radiative enhancement and the effect of variation of the ligand *trans* to the Re≡N bond on their photophysical properties, a new series of luminescent nitrido complexes $[ReNL_2X]^{n+}$ [L = dppe, X = F, Cl, Br, I, NCS, NCO or N_3 (n = 1) or MeCN (n = 2); L = dppbz($Ph_2PC_6H_4PPh_2$-*o*), X = Cl (n = 1) or MeCN (n = 2)] were synthesized. In this paper, the syntheses, spectroscopy and electrochemistry of the complexes are reported and compared with the organometallic analogues $[ReNR_2(PPh_3)_2]$ (R = C≡CBu^t or C_6H_4Me-*p*). The crystal structure of $[ReN(C{\equiv}CBu^{t})_2(PPh_3)_2]$ is described. The reactivities of some of the nitrido diphosphine complexes toward electron donors such as aromatic amines and hydrocarbons, and trifluoroacetic acid are also discussed.

Experimental

Reagents and materials

Both rhenium powder and potassium perrhenate(VII) ($KReO_4$) were purchased from Johnson Matthey Ltd. The complexes $[ReN(dppe)_2Cl]^{+}$[2d] and $[ReN(dppbz)_2Cl]^{+}$ [dppbz = 1,2-bis(diphenylphosphino)benzene],[2d] lithium *tert*-butylacetylide[5a] and *p*-tolyllithium[5b] were prepared according to literature procedures. The ligands dppe and dppbz were obtained from Strem Chemicals, Inc. Tetra-*n*-butylammonium hexafluorophosphate (NBu_4PF_6) (98%, Aldrich) was recrystallized twice from absolute ethanol and vacuum dried before use. Sodium azide (NaN_3) (Merck, 99%), sodium thiocyanate (NaSCN) (Merck, 99%), tetra-*n*-butylammonium chloride (NBu_4Cl) (Merck, 98%), potassium cyanate (KOCN) (BDH, LR), tetra-*n*-butylammonium fluoride trihydrate ($NBu_4F{\cdot}3H_2O$) (Aldrich, 99%), tetra-*n*-butylammonium bromide (NBu_4Br) (Fluka, puriss), silver trifluoromethanesulfonate $Ag(CF_3SO_3)$ (Aldrich, 99%) and trifluoroacetic acid (CF_3CO_2H) (Aldrich, 99%) were used as received. Tetra-*n*-butylammonium iodide (NBu_4I) (Fluka, puriss) and all organic quenchers (Aldrich, AR) for quenching studies were purified according to literature procedures.[6] Both acetonitrile (Ajax, AR) and dichloromethane (Ajax, AR) were distilled over calcium hydride before use. Benzene and toluene (Ajax, AR), and light petroleum (Ajax, AR, b.p. 60–80 °C) were purified by distillation under nitrogen in the presence of sodium-benzophenone. All other reagents and solvents were of analytical grade and were used as received.

Physical measurements and instrumentation

UV/VIS spectra were recorded on a Milton-Roy Spectronic 3000 diode array spectrophotometer, IR spectra as Nujol mulls on a Bio-Rad FTS-7 IR spectrometer (4000–400 cm^{-1}), Raman spectra as solid samples on a Perkin-Elmer NIR-FT-Raman 1700X spectrometer with the 1064-nm line of a Nd:YAG laser as the excitation source and ^1H and ^{31}P NMR spectra were recorded on a JEOL JNM-GSX270 Fourier-transform NMR spectrometer with chemical shifts reported relative to $SiMe_4$ and H_3PO_4, respectively. Conductivity measurements were made using a Radiometer model CDH2 conductivity meter with 0.1 mol dm^{-3} KCl as calibrant. Positive-ion FAB mass spectra were recorded on a Finnigan MAT95 mass spectrometer. Steady-state excitation and emission spectra were recorded on a Spex Fluorolog 111 spectrofluorometer. Low-temperature (77 K) spectra were recorded by using a quartz optical Dewar sample holder. The relative luminescence

quantum yield was measured by the method of Demas and Crosby[7] with $[Ru(bipy)_3][PF_6]_2$ (bipy = 2,2′-bipyridine) in degassed acetonitrile ($\Phi = 0.062$) at room temperature as the standard.[8] Luminescence quenching experiments were monitored by time-resolved (lifetime) emission measurements in MeCN (0.1 mol dm^{-3} NBu_4PF_6) and data were treated by a Stern–Volmer fit as described $\tau_0/\tau = 1 + k_q\tau_0[Q]$ where τ_0 and τ are the lifetimes in the absence and presence of quencher Q, respectively. Emission lifetime measurements were performed using a conventional laser system. The excitation source was the 355-nm output (third harmonic) of a Quanta-Ray Q-switched DCR-3 pulsed Nd-YAG laser (10 Hz, G-resonator). Luminescence decay signals were recorded on a Tektronix model 2430 digital oscilloscope, and analysed using a program for exponential fits. All solutions for photophysical and quenching studies were prepared under vacuum in a 10 cm^3 round-bottom flask equipped with a sidearm 1 cm quartz fluorescence cuvette and sealed from the atmosphere by a Kontes quick-release Teflon stopper. Solutions were rigorously degassed with no fewer than four freeze–pump–thaw cycles. The transient absorption spectra and kinetics were obtained using a conventional set-up with the output (355 nm) of a DCR-3 pulsed Nd-YAG laser as the excitation source. The monitoring beam was a 100 W tungsten lamp perpendicular to the laser beam.

Cyclic voltammetric measurements were performed by using a Princeton Applied Research (PAR) universal programmer (model 175), potentiostat (model 173), and digital coulometer (model 179) coupled to a Kipp & Zoner BD90 X-Y recorder. The ferrocenium–ferrocene couple was used as the internal standard[9] in the electrochemical measurements in acetonitrile and dichloromethane (0.1 mol dm^{-3} NBu_4PF_6). The working electrode was a glassy carbon (Atomergic Chemetals V25) electrode with a piece of platinum gauze acting as the counter electrode. Treatment of the electrode surfaces was as reported previously.[2d]

Syntheses of rhenium complexes

$[ReN(dppe)_2(MeCN)][ClO_4]_2$. A solution of $[ReN(dppe)_2Cl]ClO_4$ (0.25 g, 0.2 mmol) in acetonitrile (40 cm^3) was combined with silver trifluoromethanesulfonate (0.15 g, 0.6 mmol), and the mixture was stirred at 70 °C under an atmosphere of nitrogen for 20 min. It was filtered to remove the insoluble silver chloride and the yellow-green solid was obtained by subsequent addition of diethyl ether to the filtrate. Yellow-green crystalline samples of $[ReN(dppe)_2(MeCN)][ClO_4]_2\cdot H_2O$ were obtained by recrystallization *via* diethyl ether diffusion into an acetonitrile solution of the complex. Yield: 85% (Found: C, 51.55; H, 4.05; Cl, 4.90; N, 2.10. Calc. for $C_{54}H_{53}Cl_2N_2O_9P_4Re$: C, 51.70; H, 4.25; Cl, 5.65; N, 2.25%). IR (Nujol mull): ν(C≡N) 2295, 2265, ν(Re≡N) 1072 cm^{-1}. Raman (solid sample): ν(C≡N) 2264, ν(Re≡N) 1080 cm^{-1}. NMR (CD_3CN): ^1H, δ 2.0 (s, 3 H, MeCN), 2.6 (m, 4 H, CH_2 of dppe), 3.4 (m, 4 H, CH_2 of dppe), 6.7–7.8 (m, 40 H, aryl); ^{31}P, δ 39.0. Molar conductivity (in MeCN at 298 K) = 280 Ω^{-1} cm^2 mol^{-1}. Positive-ion FAB-MS: *m/z* 1096 $\{[(M - MeCN)ClO_4]^+\}$, 997 $\{(M - MeCN)^+\}$. UV/VIS (MeCN): λ/nm (ε_{max}/dm^3 mol^{-1} cm^{-1}) 243 (sh) (38 000), 268 (sh) (16 840), 392 (200).

$[ReN(dppe)_2F]ClO_4$. A solution of $[ReN(dppe)_2(MeCN)][ClO_4]_2$ (0.1 g, 0.08 mmol) in acetone (20 cm^3) was combined with tetra-*n*-butylammonium fluoride (0.025 g, 0.1 mmol), and the mixture was stirred at room temperature under an atmosphere of nitrogen for 1 h. It was filtered and the solvent was removed by rotary evaporation. The very pale yellow solid residue was then recrystallized from acetone–diethyl ether or acetonitrile–diethyl ether to give pale yellow needle-shaped crystals. Yield: 90% (Found: C, 55.80; H, 4.20; N, 1.10. Calc. for $C_{52}H_{48}ClFNO_4P_4Re$: C, 56.00; H, 4.35; N, 1.25%). IR (Nujol mull): ν(Re≡N) 1052 cm^{-1}. Positive-ion FAB-MS: *m/z* 1016 $\{M^+\}$, 618 $\{(M - dppe)^+\}$. UV/VIS (MeCN): λ/nm (ε_{max}/dm^3 mol^{-1} cm^{-1}) 238 (sh) (62 005), 275 (sh) (9605), 347 (345).

$[ReN(dppe)_2Br]ClO_4$. The procedure is similar to that described for the preparation of $[ReN(dppe)_2F]ClO_4$ except tetra-*n*-butylammonium bromide (0.035 g, 0.1 mmol) was used in place of tetra-*n*-butylammonium fluoride. Yield: 90% {Found: C, 53.15; H, 4.95; N, 1.75. Calc. for $[ReN(dppe)_2Br]ClO_4\cdot 0.5MeCN\cdot 0.5Et_2O$, $C_{55}H_{54.5}BrClN_{1.5}O_{4.5}P_4Re$: C, 53.55; H, 4.45; N, 1.70%}. IR (Nujol mull): ν(Re≡N) 1048 cm^{-1}. Positive-ion FAB-MS: *m/z* 1076 $\{M^+\}$, 678 $\{(M - dppe)^+\}$. UV/VIS (MeCN): λ/nm(ε_{max}/dm^3 mol^{-1} cm^{-1}) 242 (sh) (52 390), 271 (sh) (17 270), 373 (215).

$[ReN(dppe)_2I]ClO_4$. The procedure is similar to that described for the preparation of $[ReN(dppe)_2F]ClO_4$ except tetra-*n*-butylammonium iodide (0.037 g, 0.1 mmol) was used in place of tetra-*n*-butylammonium fluoride. Yield: 90% {Found: C, 50.35; H, 4.15; N, 1.00. Calc. for $[ReN(dppe)_2I]ClO_4\cdot 0.5H_2O$, $C_{52}H_{49}ClINO_{4.5}P_4Re$: C, 50.70; H, 4.00; N, 1.15%}. IR (Nujol mull): ν(Re≡N) 1043 cm^{-1}. Positive-ion FAB-MS: *m/z* 1124 $\{M^+\}$, 726 $\{(M - dppe)^+\}$. UV/VIS (MeCN): λ/nm(ε_{max}/dm^3 mol^{-1} cm^{-1}) 238 (sh) (70 110), 271 (sh) (19 005), 306 (sh) (5440), 390 (sh) (245).

$[ReN(dppe)_2(SCN)]ClO_4$. To a stirred solution of $[ReN(dppe)_2Cl]ClO_4$ (0.1 g, 0.08 mmol) in acetone (20 cm^3) was added sodium thiocyanate (0.01 g, 0.12 mmol) in water (10 cm^3) under nitrogen. The solution mixture was then stirred for 1 h and subsequent removal of acetone by rotary evaporation precipitated orange solids of $[ReN(dppe)_2(SCN)]ClO_4$, which were collected by suction filtration and recrystallized from acetonitrile–diethyl ether to give orange crystals of the complex. An alternative procedure is the reaction of $[ReN(dppe)_2Cl]ClO_4$ and sodium thiocyanate in methanol under reflux for 12 h under an atmosphere of nitrogen. Yield: 86% {Found: C, 53.95; H, 4.25; N, 2.20. Calc. for $[ReN(dppe)_2(SCN)]ClO_4\cdot H_2O$, $C_{53}H_{50}ClN_2O_5P_4ReS$: C, 54.30; H, 4.30; N, 2.40%}. IR (Nujol mull): ν_{asym}(NCS) 2025, ν(Re≡N) 1047 cm^{-1}. Positive-ion FAB-MS: *m/z* 1055 $\{M^+\}$, 657 $\{(M - dppe)^+\}$. UV/VIS (MeCN): λ/nm(ε_{max}/dm^3 mol^{-1} cm^{-1}) 276 (sh) (14 890), 383 (325), 472 (50), 528 (30).

$[ReN(dppe)_2(OCN)]ClO_4$. To a stirred solution of $[ReN(dppe)_2Cl]ClO_4$ (0.1 g, 0.08 mmol) in acetone (20 cm^3) was added potassium cyanate (0.01 g, 0.12 mmol) in water (10 cm^3) under nitrogen. The solution mixture was then stirred for 1 h and subsequent removal of acetone by rotary evaporation precipitated pale yellow solids of $[ReN(dppe)_2(OCN)]ClO_4$. The solids were collected by suction filtration and recrystallized from acetone–diethyl ether to give pale yellow crystals of the complex. Yield: 80% {Found: C, 54.80; H, 4.55; N, 1.65. Calc. for $[ReN(dppe)_2(OCN)]ClO_4\cdot 3H_2O\cdot 2Me_2CO$, $C_{59}H_{66}ClN_2O_{10}P_4Re$: C, 54.15; H, 5.10; N, 2.15%}. IR (Nujol mull): ν_{asym}(NCO) 2200, ν(Re≡N) 1038 cm^{-1}. Positive-ion FAB-MS: *m/z* 1039 $\{M^+\}$, 641 $\{(M - dppe)^+\}$. UV/VIS (MeCN): λ/nm(ε_{max}/dm^3 mol^{-1} cm^{-1}) 240 (sh) (31 390), 270 (sh) (13 120), 350 (sh) (345).

$[ReN(dppe)_2(N_3)]ClO_4$. To a stirred solution of $[ReN(dppe)_2Cl]ClO_4$ (0.1 g, 0.08 mmol) in acetone (20 cm^3) was added sodium azide (0.01 g, 0.15 mmol) in methanol (10 cm^3) under nitrogen. The solution mixture was then stirred for 1 h and subsequent addition of diethyl ether gave yellow solids. Yellow crystalline samples of $[ReN(dppe)_2(N_3)]ClO_4$ were obtained by recrystallization *via* diethyl ether diffusion into an acetone solution of the complex. Yield: 90% {Found: C, 54.25; H, 4.10; N, 4.65. Calc. for $[ReN(dppe)_2(N_3)]ClO_4\cdot 0.5H_2O$, C_{52}-

$H_{49}ClN_4O_{4.5}P_4Re$: C, 54.45; H, 4.30; N, 4.90%}. IR (Nujol mull): $\nu_{asym}(N_3)$ 2092, ν(Re≡N) 1036 cm^{-1}. Positive-ion FAB-MS: *m/z* 1039 $\{M^+\}$, 641 $\{(M - dppe)^+\}$. UV/VIS (MeCN): λ/nm(ε_{max}/dm^3 mol^{-1} cm^{-1}) 260 (sh) (21 070), 286 (sh) (9880), 363 (sh) (350).

[ReN(dppbz)$_2$(MeCN)][ClO$_4$]$_2$. A solution of [ReN(dppbz)$_2$Cl]ClO_4 (0.25g, 0.19 mmol) in acetonitrile (40 cm^3) was combined with silver trifluoromethanesulfonate (0.15 g, 0.57 mmol), and the mixture was refluxed under an atmosphere of nitrogen for 24 h. It was then filtered to remove the insoluble silver chloride and a yellow-green precipitate was obtained by subsequent addition of diethyl ether to the filtrate. Yellow-green needle-shaped crystals of [ReN(dppbz)$_2$(MeCN)][ClO_4]$_2$ were obtained by recrystallization *via* diethyl ether diffusion into an acetonitrile solution of the complex. Yield: 80% {Found: C, 53.95; H, 3.60; N, 2.05. Calc. for [ReN(dppbz)$_2$(MeCN)][ClO_4]$_2$·2H_2O, $C_{62}H_{55}Cl_2N_2O_{10}P_4Re$: C, 54.40; H, 4.05; N, 2.05%). IR (Nujol mull): ν(C≡N) 2309, 2271, ν(Re≡N) 1070 cm^{-1}. ^1H NMR (CD_3CN), δ 2.0 (s, 3 H, MeCN), 6.4–6.6 (m, 8 H, aryl protons of *o*-phenylene bridge), 7.2–7.8 (m, 40 H, aryl protons). Positive-ion FAB-MS: *m/z* 1192 $\{[(M - MeCN)ClO_4]^+\}$, 1093 $\{(M - MeCN)^+\}$. UV/VIS (MeCN): λ/nm(ε_{max}/dm^3 mol^{-1} cm^{-1}) 237 (sh) (35 060), 277 (sh) (8655), 378 (345).

[ReN(C≡CBu^t)$_2$(PPh$_3$)$_2$]. The complex was prepared by a method similar to that reported by Chatt *et al.*[10] A solution of lithium *tert*-butylacetylide (0.6 mmol) in diethyl ether (10 cm^3) was added to a stirred suspension of [$ReNCl_2(PPh_3)_2$] (0.2 g, 0.25 mmol) in toluene (40 cm^3) at room temperature. Stirring was continued for 3 h, after which the mixture was evaporated under vacuum to dryness. The orange residue was then recrystallized from toluene–light petroleum (b.p. 60–80 °C) at 0 °C to give orange microcrystals. Yield: 80% (Found: C, 64.60; H, 5.15; N, 1.45. Calc. for $C_{48}H_{48}NP_2Re$: C, 65.00; H, 5.45; N, 1.60%). IR (Nujol mull): ν(Re≡N) 1080 cm^{-1}. NMR (C_6D_6): ^1H, δ 0.9 (s, 18 H, Bu^t), 7.0 (m, 18 H, aryl protons *m* and *p* to P), 8.1 (m, 12 H, aryl protons *o* to P); ^{31}P, δ 34.6. UV/VIS (benzene): λ/nm(ε_{max}/dm^3 mol^{-1} cm^{-1}) 337 (1375), 458 (430).

[ReN(C$_6$H$_4$Me-*p*)$_2$(PPh$_3$)$_2$]. The procedure is similar to that described for the preparation of [ReN(C≡CBu^t)$_2$(PPh$_3$)$_2$] except that *p*-tolyllithium (0.6 mmol) was used in place of lithium *tert*-butylacetylide. Reddish-orange crystals of [ReN(C$_6$H$_4$Me-*p*)$_2$(PPh$_3$)$_2$] were obtained from toluene–light petroleum (b.p. 60–80 °C) solution of the crude product. Yield: 85% {Found: C, 68.35; H, 5.10; N, 1.30. Calc. for [ReN(C$_6$H$_4$Me-*p*)$_2$(PPh$_3$)$_2$]·$C_6H_5CH_3$, $C_{57}H_{52}NP_2Re$: C, 68.50; H, 5.25; N, 1.40%}. IR (Nujol mull): ν(Re≡N) 1070 cm^{-1}. NMR (C_6D_6): ^1H, δ 2.2 (s, 6 H, Me), 6.7 (m, 8 H, C_6H_4Me), 7.0 (m, 18 H, aryl protons *m* and *p* to P), 7.7 (m, 12 H, aryl protons *o* to P); ^{31}P, δ 31.9. UV/VIS (benzene): λ/nm(ε_{max}/dm^3 mol^{-1} cm^{-1}) 325 (sh) (4690), 366 (sh) (1865), 489 (1130).

Crystal structure determination

Crystals of [ReN(C≡CBu^t)$_2$(PPh$_3$)$_2$] were obtained by vapour diffusion of light petroleum (b.p. 60–80 °C) into a toluene solution of the complex.

Crystal data. $C_{48}H_{48}NP_2Re$; M = 887.07, monoclinic, space group $P2_1/n$, a = 13.708(8), b = 19.161(6), c = 17.246(3) Å, β = 109.49(4)°, U = 4270(3) $Å^3$, Z = 4, D_c = 1.380 g cm^{-3}, μ(Mo-Kα) = 29.88 cm^{-1}, F(000) = 1792, T = 298 K. A crystal of dimensions 0.20 × 0.10 × 0.30 mm was used for data collection at 25 °C on a Rigaku AFC7R diffractometer with graphite-monochromated Mo-Kα radiation (λ = 0.710 73 Å) using ω–2θ scans with ω-scan angle (0.68 + 0.35 tan θ)° at a scan speed of 16.0° min^{-1} (up to 4 scans). Intensity data (up to $2\theta_{max}$ = 45°; *h*, 0–14; *k*, 0–18; *l*, −15 to 15 and three standard reflections measured after every 300 showed decay of 3.44%) were corrected for Lorentz and polarization effects and decay correction, and empirical absorption corrections based on a ψ-scan of four strong reflections (minimum and maximum transmission factors 0.4234 and 1.0000). Upon averaging the 6089 reflections, 5809 were uniquely measured (R_{int} = 0.173). As the reflections were generally rather weak, only 1486 reflections with $I > 3\sigma(I)$ were considered observed and used in the structural analysis. The space group was determined from systematic absences and the structure solved by heavy-atom Patterson methods and expanded using Fourier techniques.[11a] Refinement by full-matrix least squares used the MSC-Crystal Structure Package TEXSAN[11b] on a Silicon Graphics Indy computer. As the number of observed reflections was small, only the Re and the two P atoms were refined anisotropically and the remaining N and C atoms were refined isotropically. Hydrogen atoms at calculated positions with thermal parameters equal to 1.3 times that of the attached C atoms were not refined. Convergence for 224 variable parameters by least squares refinement on F with $w = 4F_o^2/\sigma^2(F_o^2)$, where $\sigma^2(F_o^2) = [\sigma^2(I) + (0.020F_o^2)^2]$ for 1486 reflections with $I > 3\sigma(I)$, was reached at R = 0.053 and R' = 0.052 with a goodness-of-fit of 1.53. $(\Delta/\sigma)_{max}$ = 0.01. The final difference Fourier map was featureless, with maximum positive and negative peaks of 0.96 and 0.64 e $Å^{-3}$ respectively. The atomic coordinates of non-hydrogen atoms are collected in Table 1. Selected bond distances and angles are summarized in Table 2. Complete atomic coordinates, thermal parameters and bond lengths and angles have been deposited at the Cambridge Crystallographic Data Centre, see Instructions for Authors, *J. Chem. Soc., Dalton Trans.*, 1996, Issue 1.

Results and Discussion

Treatment of an acetonitrile solution of [ReN(dppe)$_2$Cl]ClO_4 with Ag(CF_3SO_3) at 70 °C under an atmosphere of nitrogen afforded [ReN(dppe)$_2$(MeCN)][ClO_4]$_2$ in almost quantitative yield.[2b] Reaction of [ReN(dppe)$_2$(MeCN)]$^{2+}$ with a series of halides and pseudohalides generated a series of nitrido complexes [ReN(dppe)$_2$X]$^+$ (X = F, Br, I, NCS, NCO or N_3) in high yield (85–90%), which involves simply the substitution of the labile MeCN ligand. It seems that [ReN(dppe)$_2$(MeCN)][ClO_4]$_2$ is an ideal starting material for the general synthesis. The complex [ReN(dppbz)$_2$(MeCN)]$^{2+}$ was prepared analogously by the reaction of [ReN(dppbz)$_2$Cl]$^+$ and Ag(CF_3SO_3) in acetonitrile solution except that a longer reaction time and the heating of the reaction mixture to reflux were required.

All the nitridorhenium(v) complexes are stable both in the solid state and in solution for long periods of time. [$ReNL_2X]^{n+}$ show an intense IR absorption band at *ca.* 1036–1072 cm^{-1}, assignable as the ν(Re≡N) stretch. The observed stretching frequencies are comparable to those found for other nitridorhenium(v) complexes.[1] A comparison of the solid-state Raman spectra shows that the ν(Re≡N) stretch is shifted from 1044 cm^{-1} in [ReN(dppe)$_2$Cl]$^+$ to 1080 cm^{-1} in [ReN(dppe)$_2$(MeCN)]$^{2+}$ and 1043 cm^{-1} in [ReN(dppbz)$_2$Cl]$^+$ to 1070 cm^{-1} in [ReN(dppbz)$_2$(MeCN)]$^{2+}$. This strengthening of the Re≡N bond in [ReN(dppe)$_2$(MeCN)]$^{2+}$ and [ReN(dppbz)$_2$(MeCN)]$^{2+}$ could be attributed to a more effective d_π(Re)–p_π(N) overlap due to removal of the d_π–p_π overlap between the Re and Cl atoms upon replacing Cl by MeCN and the replacement of the stronger σ donor Cl ligand by a weaker one, MeCN. The downfield shift of the ^{31}P NMR signal in [ReN(dppe)$_2$(MeCN)]$^{2+}$ (δ 39.0) relative to [ReN(dppe)$_2$Cl]$^+$ (δ 27.9) is in accord with the lower electron density at the Re centre in the former which withdraws electron density from the phosphorus donor atoms which are thus deshielded. The variation of ν(Re≡N) in the series of

Table 1 Atomic parameters for $[ReN(C{\equiv}CBu^t)_2(PPh_3)_2]$ with estimated standard deviations (e.s.d.s) in parentheses

Atom	*x*	*y*	*z*	Atom	*x*	*y*	*z*
Re	0.152 2(1)	0.221 84(8)	0.453 31(8)	C(23)	−0.053(2)	0.291(2)	0.643(2)
P(1)	0.098 3(6)	0.336 9(4)	0.480 7(5)	C(24)	−0.008(2)	0.289(2)	0.580(2)
P(2)	0.170 0(6)	0.126 4(4)	0.367 0(5)	C(25)	−0.006(2)	0.367(1)	0.388(2)
N	0.220(2)	0.190(1)	0.542(1)	C(26)	0.011(2)	0.366(1)	0.317(2)
C(1)	0.003(2)	0.194(1)	0.420(2)	C(27)	−0.071(2)	0.387(1)	0.243(2)
C(2)	−0.090(2)	0.185(1)	0.393(2)	C(28)	−0.157(2)	0.412(2)	0.250(2)
C(3)	−0.205(2)	0.170(2)	0.353(2)	C(29)	−0.173(2)	0.416(2)	0.322(2)
C(4)	−0.243(3)	0.214(2)	0.276(2)	C(30)	−0.093(2)	0.394(2)	0.396(2)
C(5)	−0.261(3)	0.209(2)	0.404(2)	C(31)	0.124(2)	0.154(1)	0.259(2)
C(6)	−0.234(3)	0.096(2)	0.347(2)	C(32)	0.183(2)	0.138(2)	0.208(2)
C(7)	0.247(2)	0.276(2)	0.404(1)	C(33)	0.146(3)	0.167(2)	0.128(2)
C(8)	0.294(2)	0.310(1)	0.368(2)	C(34)	0.060(3)	0.207(2)	0.102(2)
C(9)	0.351(2)	0.349(2)	0.327(2)	C(35)	0.004(2)	0.225(2)	0.152(2)
C(10)	0.359(3)	0.425(2)	0.350(2)	C(36)	0.032(2)	0.195(1)	0.230(2)
C(11)	0.455(2)	0.318(2)	0.340(2)	C(37)	0.301(2)	0.090(1)	0.389(2)
C(12)	0.293(2)	0.345(2)	0.235(2)	C(38)	0.313(3)	0.027(2)	0.353(2)
C(13)	0.193(2)	0.407(1)	0.502(2)	C(39)	0.409(3)	0.005(2)	0.364(2)
C(14)	0.291(2)	0.395(2)	0.555(2)	C(40)	0.496(2)	0.042(2)	0.407(2)
C(15)	0.371(2)	0.446(2)	0.573(2)	C(41)	0.485(3)	0.104(2)	0.441(2)
C(16)	0.339(3)	0.511(1)	0.540(2)	C(42)	0.381(2)	0.130(1)	0.425(2)
C(17)	0.242(2)	0.523(2)	0.489(2)	C(43)	0.096(2)	0.046(1)	0.369(2)
C(18)	0.169(2)	0.473(2)	0.470(2)	C(44)	0.113(3)	0.010(2)	0.438(2)
C(19)	0.044(2)	0.347(1)	0.566(2)	C(45)	0.053(3)	−0.047(2)	0.445(2)
C(20)	0.051(2)	0.406(2)	0.609(2)	C(46)	−0.016(3)	−0.069(2)	0.376(3)
C(21)	0.009(2)	0.409(2)	0.673(2)	C(47)	−0.035(2)	−0.036(2)	0.305(2)
C(22)	−0.043(2)	0.353(2)	0.685(2)	C(48)	0.019(2)	0.025(2)	0.300(2)

Table 2 Selected bond distances (Å) and angles (°) for $[ReN(C{\equiv}CBu^t)_2(PPh_3)_2]$ with e.s.d.s in parentheses

Re–N	1.63(2)	Re–C(7)	2.06(3)
Re–P(1)	2.422(8)	C(1)–C(2)	1.21(3)
Re–P(2)	2.421(8)	C(7)–C(8)	1.22(3)
Re–C(1)	2.01(2)	P–C(Ph)	1.82(3)–1.87(3)
P(1)–Re–P(2)	155.2(3)	P(2)–Re–C(7)	85.3(8)
P(1)–Re–N	105.9(7)	C(1)–Re–C(7)	138.1(9)
P(1)–Re–C(1)	87.1(7)	N–Re–C(1)	111(1)
P(1)–Re–C(7)	84.2(8)	N–Re–C(7)	110.0(9)
P(2)–Re–N	98.8(8)	Re–C(1)–C(2)	170(2)
P(2)–Re–C(1)	85.8(7)	Re–C(7)–C(8)	173(2)

$[ReN(dppe)_2X]^+$ complexes is small and is close to the value of ν(Re≡N) for $[ReN(dppe)_2Cl]^+$ (1044 cm^{-1}), but lower than those of $[ReN(C{\equiv}CBu^t)_2(PPh_3)_2]$ (1080 cm^{-1}) and $[ReN(C_6H_4Me\text{-}p)_2(PPh_3)_2]$ (1070 cm^{-1}).

Fig. 1 depicts the perspective drawing of $[ReN(C{\equiv}CBu^t)_2(PPh_3)_2]$ with atomic numbering. The structure resembles those of $[ReN(Me)_2(PPh_3)_2]$[2c] and the chloro analogue $[ReNCl_2(PPh_3)_2]$[1] in having a distorted trigonal-bipyramidal geometry, with a Re≡N distance of 1.63(2) Å, which is similar to that found in $[ReN(Me)_2(PPh_3)_2]$ [1.641(4) Å][2c] and $[ReNCl_2(PPh_3)_2]$ [1.602(9) Å],[1] but shorter than that of $[ReN(dpae)_2Cl]^+$ [dpae = 1,2-bis(diphenylarsino)ethane] [1.839(8) Å],[2d] which could be attributed to the relief of the steric effects from an octahedral to a trigonal-bipyramidal geometry. The Re–P distances of 2.422(8) and 2.421(8) Å compares favourably with those found in the chloro analogues.[1] In $[ReN(C{\equiv}CBu^t)_2(PPh_3)_2]$, the arrangements of the Re–C≡CBu^t moiety are almost linear and the C≡C bond distances are typical of terminal acetylides. All other bond distances and angles are normal.

The UV/VIS absorption spectra of the nitrido complexes $[ReNL_2X]^{n+}$ in acetonitrile exhibit intense absorption bands in the region 230–300 nm and a weak absorption at *ca.* 345–395 nm (ε ≈ 210–350 $dm^3\ mol^{-1}\ cm^{-1}$) with very weak shoulders tailing in the region 400–550 nm (ε < 100). The large absorption coefficients observed for the bands at *ca.* 240 and 270 nm possibly suggest their origins as intraligand transition

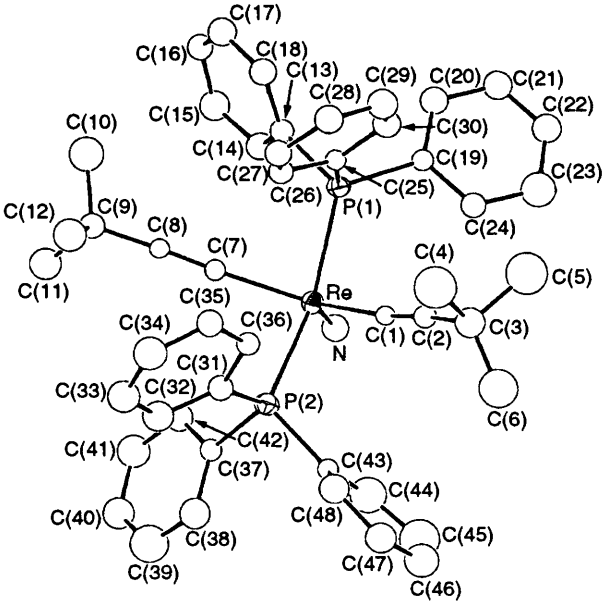

Fig. 1 Perspective drawing of $[ReN(C{\equiv}CBu^t)_2(PPh_3)_2]$ showing the atomic numbering scheme. Thermal ellipsoids are shown at the 25% probability level

and ligand-to-metal charge-transfer (l.m.c.t.) transitions $[p_\pi(N^{3-}) \longrightarrow d_{\pi^*}(Re)$ and/or $p_\pi(X) \longrightarrow d_{\pi^*}(Re)$, $d_{\pi^*} = d_{xz}, d_{yz}]$, respectively. An additional band at *ca.* 305 nm is uniquely observed in the complex $[ReN(dppe)_2I]ClO_4$. It is likely that the 305 nm band in $[ReN(dppe)_2I]^+$ is derived from a l.m.c.t. $[p_\pi(I) \longrightarrow d_{\pi^*}(Re)]$ origin. Thus the band at *ca.* 270 nm which occurs in all the complexes is possibly derived from l.m.c.t. $[p_\pi(N^{3-}) \longrightarrow d_{\pi^*}(Re)]$ transition. In the other nitrido complexes, the $p_\pi(X)$ is lower lying in energy than the $p_\pi(I)$ based on their optical electronegativities[12] and hence their l.m.c.t. $[p_\pi(X) \longrightarrow d_{\pi^*}(Re)]$ transitions are expected to occur at higher energy than that of the iodide case. Therefore, it is likely that the band at *ca.* 270 nm in other nitrido complexes may be tentatively assigned as admixtures of l.m.c.t. $[p_\pi(N^{3-}) \longrightarrow d_{\pi^*}(Re)]$ and l.m.c.t. $[p_\pi(X) \longrightarrow d_{\pi^*}(Re)]$ transitions. In

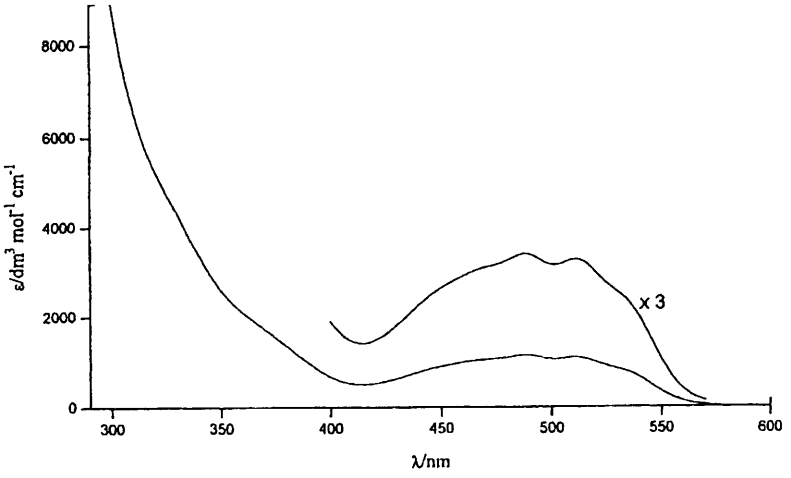

Fig. 2 Electronic absorption spectrum of $[ReN(C_6H_4Me\text{-}p)_2(PPh_3)_2]$ in benzene at 298 K

the case of X = F, the 270 nm band is assigned as a pure l.m.c.t. $[p_\pi(N^{3-}) \longrightarrow d_{\pi^*}(Re)]$ transition given the extremely high energy of the l.m.c.t. $[p_\pi(F) \longrightarrow d_{\pi^*}(Re)]$ transition. A similar shift in the l.m.c.t. $[p_\pi(X) \longrightarrow d_{\pi^*}(Re)]$ transition energies has also been observed in the series $[ReN(dmpe)_2X]^+$ (dmpe = $Me_2PCH_2CH_2PMe_2$),[4h] where the l.m.c.t. bands occur at 240 nm (X = Cl), 248 nm (X = Br), 262 nm (X = N_3) and 264 nm (X = I). With reference to previous spectroscopic works on d^2 metal nitrido system,[2,4] the energies of d orbitals of Re≡N complexes, assuming a C_{2v} symmetry are in the order $a_2(d_{xy}) < b_1(d_{xz}) \approx b_2(d_{yz}) < a_1(d_{x^2-y^2}) < a_1(d_{z^2})$. The weak absorption in the low-energy region is likely to be derived from the $(d_{xy})^2 \longrightarrow (d_{xy})^1(d_{yz})^1$ $(A_1 \longrightarrow B_1)$ and $(d_{xy})^2 \longrightarrow (d_{xy})^1(d_{xz})^1$ $(A_1 \longrightarrow B_2)$ transitions. Comparison of the electronic absorption spectral data for a series of $[ReN(dppe)_2X]^+$ where X = F (347 nm), Cl (369 nm), Br (373 nm), I (390 nm) shows that the position of the d–d absorption band is strongly dependent on the identity of the halide ligand. The spectral shift of the d–d absorption band may be explained in terms of the combined effect of $p_\pi(N^{3-})$–$d_\pi(Re)$ and $p_\pi(X)$–$d_\pi(Re)$ (X = F, Cl, Br, I and $d_\pi = d_{xz}$, d_{yz}) overlap on the energy separation of the d_{xy} and d_{xz}, d_{yz} orbitals, where the π-donating ability of X is found to decrease down the group. A separate study on the electronic structure of the *trans*-$[WE_2(PMe_3)_4]$ complexes (E = S, Se or Te)[13] showed that the energy of the $d_{xy} \longrightarrow d_{\pi^*}$ transition increases in the order of Te < Se < S, in line with the increasing strength of the W–E π bond from Te to S. An alternative rationale for the observed trend in the $d_{xy} \longrightarrow d_{\pi^*}$ absorption energies is that the fluoro group being most electronegative will render the Re centre most electron deficient, thereby enhancing the $p_\pi(N^{3-})$–$d_\pi(Re)$ overlap, leading to a larger d_{xy}–d_{xz}, d_{yz} energy separation. Moreover, it is found that the d–d absorption bands of $[ReN(dppe)_2(MeCN)]^{2+}$ (392 nm) and $[ReN(dppbz)_2(MeCN)]^{2+}$ (378 nm) are red shifted relative to the corresponding bands at 369 and 360 nm in their respective chloro analogues, $[ReN(dppe)_2Cl]^+$ and $[ReN(dppbz)_2Cl]^+$. This is in accordance with the removal of the d_π–p_π overlap between the Re and Cl atoms on replacing Cl by MeCN since such an overlap would raise the energies of the d_{xz} and d_{yz} orbitals. Addition of NBu_4Cl to an acetonitrile solution of $[ReN(dppe)_2(MeCN)]^{2+}$ regenerates $[ReN(dppe)_2Cl]^+$, characterized spectroscopically by the disappearance of the 392 nm band and the appearance of the 369 nm band. On the other hand, the electronic absorption spectra of $[ReN(C{\equiv}CBu^t)_2(PPh_3)_2]$ and $[ReN(C_6H_4Me\text{-}p)_2(PPh_3)_2]$ (Fig. 2) exhibit absorption bands in the 400–550 nm region which are vibronically structured with progressional spacings of *ca.* 800–920 cm^{-1}. Similar progressions have been observed in the low-temperature absorption spectrum of $[OsNCl_4]^-$.[4a,b] This is suggestive of a weakened Re≡N bond in the excited state as a result of the promotion of an electron upon UV/VIS irradiation to the d_{xz}, d_{yz} orbitals which are π-antibonding in nature. The lower absorption energies of the organonitrido complexes than that of $[ReNL_2X]^{n+}$ are indicative of a smaller energy separation between the d_{xy} and d_{π^*} levels in the organometallic complexes. This could be attributed to the strong σ-donating effect of the alkyl groups, rendering the Re centre less electron deficient, which would lead to the lowering of the nitrogen-rhenium p_π–d_π overlap.

Excitation of solid samples of the $[ReNL_2X]^{n+}$ complexes at 350–380 nm at room temperature or 77 K results in intense yellow-green emission, and they have also been shown to exhibit long-lived room-temperature luminescence in acetonitrile solutions. On the other hand, excitation of solid samples of $[ReNR_2(PPh_3)_2]$ at λ > 400 nm gave rise to red emission, with $[ReN(C{\equiv}CBu^t)_2(PPh_3)_2]$ also being shown to exhibit room-temperature luminescence in degassed benzene solution. The excitation and emission spectra of $[ReN(dppbz)_2(MeCN)]^{2+}$ in MeCN are depicted in Fig. 3. The photophysical data are summarized in Table 3. The excitation spectra of the nitrido complexes $[ReNL_2X]^{n+}$ and $[ReNR_2(PPh_3)_2]$ show broad bands at *ca.* 315 and 400 nm and 450–550 nm, respectively. Given the long excited-state lifetime and our previous spectroscopic studies of d^2 metal nitrido systems,[2] the emissive state is likely to be derived from the $(d_{xy})^1(d_{xz})^1$ $[^3B_2]$ and $(d_{xy})^1(d_{yz})^1$ $[^3B_1]$ triplets assuming a C_{2v} symmetry. The excitation bands at *ca.* 315 and 400 nm are tentatively attributed to the $^1[(d_{xy})^2] \longrightarrow {}^1[(d_{xy})^1(d_{\pi^*})^1]$ (singlet-singlet) and $^1[(d_{xy})^2] \longrightarrow {}^3[(d_{xy})^1(d_{\pi^*})^1]$ (singlet–triplet) transitions, respectively. The emission maximum is found to shift in the same direction as the spectral shift in the d–d absorption band of the complexes $[ReN(dppe)_2X]^+$ (X = F, Cl, Br or I), and could be interpreted in the same way as the absorption spectral shift. The lower emission energy of the organometallic nitrido complexes than that of $[ReNL_2X]^{n+}$ is also consistent with the red shift in their d–d absorption bands. The luminescence quantum yields (Φ_{lum}) of the complexes $[ReN(dppe)_2X]^+$ (X = F, Cl, Br, I, NCS, N_3 or NCO) are in the range of 10^{-4}–10^{-5}. Unlike $[ReN(dppe)_2Cl]^+$ where the Φ_{lum} is very small ($\approx 10^{-5}$), the Φ_{lum} value of 0.021 in $[ReN(dppe)_2(MeCN)]^{2+}$ is greater by a factor of 10^3 than its chloro counterpart. Similarly, the Φ_{lum} value of 0.063 in $[ReN(dppbz)_2(MeCN)]^{2+}$ is greater by a factor of ≈200 than its chloro counterpart, $[ReN(dppbz)_2Cl]^+$. It is interesting that a simple replacement of the chloro ligand by MeCN improves both the luminescence quantum yield and the radiative lifetime, which may arise from the removal of the ligand-to-metal charge transfer excited state $[p_\pi(Cl) \longrightarrow 5d_{\pi^*}(Re)]$ from $[ReNL_2Cl]^+$ to $[ReNL_2(MeCN)]^{2+}$. However, the observation that $[ReN(dppe)_2(MeCN)]^{2+}$ has a larger

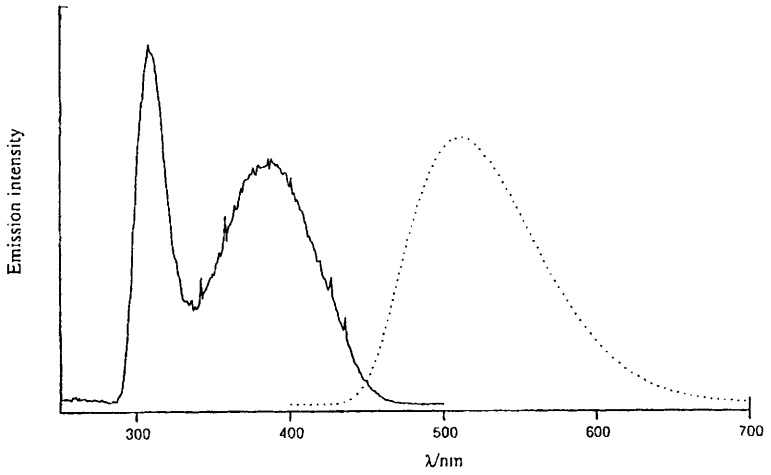

Fig. 3 Excitation (—) and emission (·····) spectra of $[ReN(dppbz)_2(MeCN)][ClO_4]_2$ in degassed MeCN at 298 K

Table 3 Photophysical data for nitridorhenium(v) complexes

Complex	Medium (T/K)	λ_{em}/nm (τ_o/μs)	Φ_{lum}*
$[ReN(dppe)_2F]^+$	Solid (298)	482 (0.80 ± 0.08)	
	Solid (77)	477	
	MeCN (298)	479 (0.35 ± 0.04)	
$[ReN(dppe)_2Cl]^+$	Solid (298)	509 (2.0 ± 0.2)	
	Solid (77)	509	
	MeCN (298)	507 (0.10 ± 0.01)	$\approx 10^{-5}$
$[ReN(dppe)_2Br]^+$	Solid (298)	515 (7.5 ± 0.8)	
	Solid (77)	511	
	MeCN (298)	498 (0.35 ± 0.05)	
$[ReN(dppe)_2I]^+$	Solid (298)	525 (3.3 ± 0.3)	
	Solid (77)	522	
	MeCN (298)	534 (0.30 ± 0.03)	
$[ReN(dppe)_2(SCN)]^+$	Solid (298)	513 (0.70 ± 0.10)	
	Solid (77)	517	
	MeCN (298)	520 (0.05 ± 0.01)	
	EtOH–MeOH–CH_2Cl_2 Glass (4 : 1 : 1 v/v)	503	
$[ReN(dppe)_2(OCN)]^+$	Solid (298)	505 (2.7 ± 0.3)	
	Solid (77)	515	
	MeCN (298)	508 (1.9 ± 0.2)	
$[ReN(dppe)_2(N_3)]^+$	Solid (298)	597 (5.4 ± 0.5)	
	Solid (77)	520	
	MeCN (298)	516 (1.6 ± 0.2)	
	EtOH–MeOH–CH_2Cl_2 Glass (4 : 1 : 1 v/v)	501	
$[ReN(dppbz)_2Cl]^+$	Solid (298)	510 (1.7 ± 0.2)	
	Solid (77)	512	
	MeCN (298)	517 (11.3 ± 1.0)	3.5×10^{-4}
$[ReN(dppe)_2(MeCN)]^{2+}$	Solid (298)	510 (18 ± 2)	
	Solid (77)	505	
	MeCN (298)	525 (2.4 ± 0.2)	0.021
$[ReN(dppbz)_2(MeCN)]^{2+}$	Solid (298)	510 (25 ± 2)	
	Solid (77)	513	
	MeCN (298)	512 (20 ± 2)	0.063
$[ReN(C{\equiv}CBu^t)_2(PPh_3)_2]$	Solid (298)	720 (6.5 ± 0.6)	
	Solid (77)	715	
	Benzene (298)	809	
$[ReN(C_6H_4Me\text{-}p)_2(PPh_3)_2]$	Solid (298)	650	

* Measured using $[Ru(bipy)_3]^{2+}$ as standard.

Φ_{lum} value than $[ReN(dppe)_2F]^+$ suggests that the raising of the energy of the l.m.c.t. excited state may not be the sole reason for the enhanced luminescence. The improved photophysical properties may also be related to the change of the geometry of the complex $[ReNL_2Cl]^+$ from a six-co-ordinate octahedron to a highly distorted pseudo-octahedron approaching five-co-ordination for $[ReNL_2(MeCN)]^{2+}$ as a result of replacing the stronger σ donor, Cl^- by MeCN. Such changes in the co-ordination geometry have also been reported by Shapley *et al.*,[14] where the structure of $[OsN(CH_2SiMe_3)_2(dppe)(MeCN)]^+$ has been shown to be very similar to that of the five-co-ordinate alkylnitridoosmium(VI) complexes, with a pronounced distortion of the equatorial ligands away from the axial nitride and with a very weak MeCN–metal interaction.

Quenching of the emission intensity of the excited-state of complexes $[ReN(dppbz)_2Cl]^+$, $[ReN(dppe)_2(MeCN)]^{2+}$ and $[ReN(dppbz)_2(MeCN)]^{2+}$ was observed for CF_3CO_2H with quenching rate constants of *ca.* 1.0×10^8, 6.0×10^7 and 2.9×10^7 $dm^3\ mol^{-1}\ s^{-1}$, respectively. The substantial

Table 4 Rate constants for quenching of the $^3[(d_{xy})^1(d_{\pi^*})^1]$ excited state of $[ReN(dppe)_2(MeCN)]^{2+}$ and $[ReN(dppbz)_2(MeCN)]^{2+}$ by organic donors in acetonitrile at 298 K

Quencher	$E_{1/2}(Q^{+/0})$ (V *vs.* NHE)[a]	$[ReN(dppe)_2(MeCN)]^{2+}$ k_q'[b]/dm^3 mol^{-1} s^{-1}	$[ReN(dppbz)_2(MeCN)]^{2+}$ k_q'[b]/dm^3 mol^{-1} s^{-1}
N,*N*,*N*′,*N*′-Tetramethyl-1,4-phenylenediamine	0.34	2.57×10^{10}	5.10×10^{10}
N,*N*,*N*′,*N*′-Tetramethylbenzidine	0.56	2.65×10^{10}	2.59×10^{10}
Diphenylamine	1.07	1.81×10^{9}	4.40×10^{9}
Triphenylamine	1.10	2.55×10^{9}	6.72×10^{9}
1,2,4-Trimethoxybenzene	1.36	6.09×10^{7}	2.65×10^{8}
1,4-Dimethoxybenzene	1.58	7.17×10^{5}	1.10×10^{7}
1,2,3-Trimethoxybenzene	1.66	$< 10^5$	1.69×10^{5}
1,3,5-Trimethoxybenzene	1.73	$< 10^5$	$< 10^5$

[a] Ref. 15, NHE = normal hydrogen electrode. [b] k_q' Refers to diffusion-corrected value, $1/k_q' = 1/k_q - 1/k_d$ where $k_d = 2.1 \times 10^{10}$ dm^3 mol^{-1} s^{-1}.

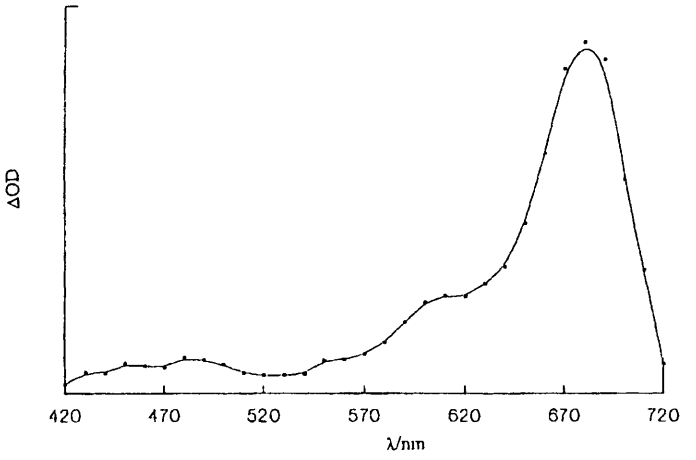

Fig. 4 Transient difference absorption spectrum recorded 3 μs after the laser flash for a degassed MeCN solution of $[ReN(dppe)_2(MeCN)][ClO_4]_2$ and dpa

attenuation of the emission intensity in the presence of acids is believed to be due to the protonation of the excited-state.[3f,g,4j] Under similar conditions, no protonation of the ground state at these acid concentrations was observed as shown by the absence of spectral changes in the absorption spectra of the complexes upon addition of the acid. The quenching rate constants for the complexes by CF_3CO_2H increase in the order: $[ReN(dppbz)_2(MeCN)]^{2+} < [ReN(dppe)_2(MeCN)]^{2+} < [ReN(dppbz)_2Cl]^{+}$, which implies the dependence of the excited-state protonation upon the composition of the co-ordination sphere around the ReN^{2+} core. The variation of the quenching rate constants for these complexes is related to the electron-richness of the complexes which also increases in the same trend. Similar variations are also observed in the *trans*-dioxorhenium(v) system[3g] with the pK_a^* value varied from $[ReO_2(3Cl\text{-}py)_4]^{+}$ (11.0) to $[ReO_2(py)_4]^{+}$ (py = pyridine) (11.3) to $[ReO_2(4OMe\text{-}py)_4]^{+}$ (12.5). The quenching rate constant of $[ReN(dppe)_2(MeCN)]^{2+}$ by benzoic acid is determined to be $< 10^6$ dm^3 mol^{-1} s^{-1} which is much smaller than that of $[ReO_2(py)_4]^{+}$ (1.3×10^9 dm^3 mol^{-1} s^{-1}).[3f,g] This difference is also reflected by the ΔpK_a for $[ReO_2(py)_4]^{+*}$ [3g] of 11 units which is much larger than that of 5 units observed for $[ReN(dmpe)_2Cl]^{+*}$.[4j] It is apparent that the excited state of the nitrido complexes is far more basic than the ground state. The increase in basicity in the excited state is due to the excitation of an electron from the essentially metal-localized (d_{xy}) orbital to the (d_{xz}, d_{yz}) orbitals which are π antibonding in nature, resulting in the lowering of the Re–N bond order while placing more electron density on nitrogen relative to the ground state.

It is found that the phosphorescence of $[ReN(dppe)_2(MeCN)]^{2+*}$ and $[ReN(dppbz)_2(MeCN)]^{2+*}$ in acetonitrile is quenched by alkoxybenzenes and organic amines. The measured rate constants corrected for the diffusion-controlled rates of luminescence quenching of $[ReN(dppe)_2(MeCN)]^{2+*}$ and $[ReN(dppbz)_2(MeCN)]^{2+*}$ by the organic quenchers are given in Table 4. The dependence of the rate constants upon the oxidation potential of the organic quenchers suggests that electron transfer is the predominant luminescence quenching mechanism for both $[ReN(dppe)_2(MeCN)]^{2+*}$ and $[ReN(dppbz)_2(MeCN)]^{2+*}$ by organic electron donors. This is consistent with our prediction that energy transfer does not contribute to a significant extent since the triplet energies of the quenchers are too high for energy transfer to be competitive with reductive electron-transfer quenching. Further evidence for electron-transfer quenching is supported by the observation of a transient signal due to the diphenylamine (dpa) cation radical (λ_{max} at *ca.* 680 nm)[16] during the laser flash photolysis of $[ReN(dppe)_2(MeCN)]^{2+}$ and dpa in degassed acetonitrile (Fig. 4). Laser flash photolysis of a degassed acetonitrile solution of $[ReN(dppe)_2(MeCN)]^{2+}$ and triphenylamine (tpa) also generated transient absorption at *ca.* 650 nm, attributable to the tpa cation radical.[16] Similarly, transient absorptions are also observed at *ca.* 680, 470 and 570 and 620 nm during the laser flash photolysis of $[ReN(dppbz)_2(MeCN)]^{2+}$ with dpa, *N*,*N*,*N*′,*N*′-tetramethylbenzidine (tmbz) and *N*,*N*,*N*′,*N*′-tetramethyl-1,4-phenylenediamine (tmpd), which are attributed to the respective cation radical of dpa, tmbz and tmpd.[16] The mechanism of the reactions is as given in Scheme 1.

$$[Re^{V}] + h\nu \longrightarrow [Re^{V}]^*$$

$$[Re^{V}]^* + D \longrightarrow [Re^{IV}] + D^{\cdot+}$$

Scheme 1 D = dpa, tpa, tmbz or tmpd; $[Re^V]$ = $[ReN(dppe)_2(MeCN)]^{2+}$ or $[ReN(dppbz)_2(MeCN)]^{2+}$

Table 5 Cyclic voltammetric data for nitridorhenium(v) complexes[a]

Complex	E_{pc}[b]/V	E_{pa}[c]/V
$[ReN(dppe)_2Cl]^+$	−2.26	+1.46
$[ReN(dppe)_2F]^+$	—	+1.43
$[ReN(dppe)_2Br]^+$	−2.20	+1.55
$[ReN(dppe)_2I]^+$	−2.06	+1.84
$[ReN(dppe)_2(SCN)]^+$	−2.14	+1.54
$[ReN(dppe)_2(OCN)]^+$	−2.29	+1.42
$[ReN(dppe)_2(N_3)]^+$	−2.27	+1.34
$[ReN(dppbz)_2Cl]^+$	−2.26	+1.57
$[ReN(dppe)_2(MeCN)]^{2+}$	−1.67, −2.26	+1.85
$[ReN(dppbz)_2(MeCN)]^{2+}$	−1.63, −2.21	+1.73
$[ReN(C{\equiv}CBu^t)_2(PPh_3)_2]$	—	+0.03[d]
$[ReN(C_6H_4Me\text{-}p)_2(PPh_3)_2]$	—	−0.18[d]

[a] In acetonitrile (0.1 mol dm^{-3} NBu_4PF_6). Working electrode: glassy carbon; scan rate, 100 mV s^{-1}; potentials quoted relative to the ferrocenium–ferrocene couple. [b] E_{pc} is the peak cathodic potential for the irreversible couple. [c] E_{pa} is the peak anodic potential for the irreversible couple. [d] In dichloromethane (0.1 mol dm^{-3} NBu_4PF_6), $E_{\frac{1}{2}}$ is taken to be the average value of the corresponding anodic and cathodic peak potentials.

Cyclic voltammetric studies show that the $[ReN(dppe)_2X]^+$ complexes display an irreversible reduction couple at E_{pc} of *ca.* −2.0 to −2.3 V and an irreversible oxidation couple at E_{pa} of *ca.* +1.3 to +1.8 V *vs.* ferrocenium–ferrocene couple in MeCN (0.1 mol dm^{-3} NBu_4PF_6). The cyclic voltammograms of $[ReN(dppe)_2(MeCN)]^{2+}$ and $[ReN(dppbz)_2(MeCN)]^{2+}$ in acetonitrile (0.1 mol dm^{-3} NBu_4PF_6) display irreversible reduction couples at E_{pa} of *ca.* − 2.26, −1.67 V and −2.21, −1.63 V, respectively and irreversible oxidation couples at E_{pa} of *ca.* +1.85 and +1.73 V, respectively *vs.* the ferrocenium–ferrocene couple. All the electrochemical data of the complexes are summarized in Table 5. Addition of NBu_4Cl to an acetonitrile solution of $[ReN(dppe)_2(MeCN)]^{2+}$ gave a cyclic voltammogram identical to that of the chloro counterpart, $[ReN(dppe)_2Cl]^+$ (E_{pc} −2.34 V; E_{pa} +1.55 V *vs.* ferrocenium–ferrocene couple). It is likely that the reduction waves at *ca.* −1.67 and −1.63 V in the respective $[ReN(dppe)_2(MeCN)]^{2+}$ and $[ReN(dppbz)_2(MeCN)]^{2+}$ complexes which are absent in the chloro analogues, correspond to the reduction processes $Re^V + e^- \longrightarrow Re^{IV}$. The anodic shift of the $E°[Re^V\text{–}Re^{IV}]$ couples in $[ReNL_2(MeCN)]^{2+}$ (L = dppe or dppbz) relative to $[ReNL_2Cl]^+$ is in accord with the stronger σ-donating ability of Cl^- over MeCN as well as the greater overall positive charge of $[ReNL_2(MeCN)]^{2+}$. The irreversible reduction and oxidation waves at *ca.* −2.0 to −2.3 V and +1.3 to +1.8 V, respectively, are likely to be ligand centred in nature. Unlike the non-organo complexes $[ReNL_2X]^{n+}$, $[ReN(C{\equiv}CBu^t)_2(PPh_3)_2]$ and $[ReN(C_6H_4Me\text{-}p)_2(PPh_3)_2]$ display a quasi-reversible one-electron oxidation couple at +0.03 and −0.18 V, respectively *vs.* the ferrocenium–ferrocene couple in CH_2Cl_2 (0.1 mol dm^{-3} NBu_4PF_6). No reduction couples were observed up to −2.50 V. The quasi-reversible oxidation is assigned as the $Re^{VI}\text{–}Re^V$ couple. The relative ease of oxidizing Re^V to Re^{VI} and the successful observation of a relatively stable rhenium(VI) species on the cyclic voltammetric timescale in the uncharged nitridorhenium(V) organometallics compared to the positively charged species $[ReNL_2X]^{n+}$ could be partially attributed to the charge effect. Moreover, the introduction of organo functionalities inevitably stabilizes the more electron-deficient d^1 rhenium(VI) species.

In conclusion, with the introduction of organo functionalities, the $[ReNR_2(PPh_3)_2]$ complexes have been shown to possess very different electrochemical and spectroscopic properties compared to those of the non-organo counterparts. In addition, the present work demonstrates that the luminescent properties of the $[ReNL_2X]^{n+}$ complexes are greatly enhanced upon substitution of the chloro ligand *trans* to the Re≡N group by a weaker σ donor, such as MeCN. Both of the findings demonstrate the wide capabilities and effectiveness of the tuning of spectroscopic, photophysical and redox properties *via* the variation of the ligands around the Re≡N core.

Acknowledgements

V. W.-W. Y. acknowledges financial support from the Research Grants Council, the Croucher Foundation and The University of Hong Kong. K.-K. T. acknowledges the receipt of a postgraduate studentship, administered by The University of Hong Kong.

References

1 W. A. Nugent and J. M. Mayer, *Metal-Ligand Multiple Bonds*, Wiley, New York, 1988.
2 (*a*) V. W. W. Yam, K. K. Tam and K. K. Cheung, *J. Chem. Soc., Dalton Trans.*, 1995, 2779; (*b*) V. W. W. Yam and K. K. Tam, *J. Chem. Soc., Dalton Trans.*, 1994, 391; (*c*) V. W. W. Yam, K. K. Tam and T. F. Lai, *J. Chem. Soc., Dalton Trans.*, 1993, 651; (*d*) V. W. W. Yam, K. K. Tam, M. C. Cheng, S. M. Peng and Y. Wang, *J. Chem. Soc., Dalton Trans.*, 1992, 1717.
3 (*a*) J. R. Winkler and H. B. Gray, *J. Am. Chem. Soc.*, 1983, **105**, 1373; (*b*) J. R. Winkler and H. B. Gray, *Inorg. Chem.*, 1985, **24**, 346; (*c*) H. H. Thorp, J. Van Houten and H. B. Gray, *Inorg. Chem.*, 1989, **28**, 889; (*d*) J. C. Brewer, H. H. Thorp, K. M. Slagle, G. W. Brudvig and H. B. Gray, *J. Am. Chem. Soc.*, 1991, **113**, 3171; (*e*) J. C. Brewer and H. B. Gray, *Preprints: Symposium on Selective Catalytic Oxidation of Hydrocarbons, ACS Division of Petroleum Chemistry*, American Chemical Society, Washington, DC, 1990, pp. 187–191; (*f*) W. Liu, T. W. Welch and H. H. Thorp, *Inorg. Chem.*, 1992, **31**, 4045; (*g*) W. Liu and H. H. Thorp, *Inorg. Chem.*, 1994, **33**, 1026.
4 (*a*) C. D. Cowman, W. C. Trogler, K. R. Mann, C. K. Poon and H. B. Gray, *Inorg. Chem.*, 1976, **15**, 1747; (*b*) M. D. Hopkins, V. M. Miskowski and H. B. Gray, *J. Am. Chem. Soc.*, 1986, **108**, 6908; (*c*) C. M. Che, V. W. W. Yam, K. C. Cho and H. B. Gray, *J. Chem. Soc., Chem. Commun.*, 1987, 948; (*d*) V. W. W. Yam, C. M. Che and W. T. Tang, *J. Chem. Soc., Chem. Commun.*, 1988, 100; (e) C. M. Che, T. C. Lau, H. W. Lam and C. K. Poon, *J. Chem. Soc., Chem. Commun.*, 1989, 114; (*f*) C. M. Che, H. W. Lam and T. C. W. Mak, *J. Chem. Soc., Chem. Commun.*, 1989, 1529; (*g*) G. A. Neyhart, M. Bakir, J. Boaz, W. J. Vining and B. P. Sullivan, *Coord. Chem. Rev.*, 1991, **111**, 27; (*h*) G. A. Neyhart, K. J. Seward, J. Boaz and B. P. Sullivan, *Inorg. Chem.*, 1991, **30**, 4486; (*i*) C. M. Che, Y. P. Wang, K. S. Yeung, K. Y. Wong and S. M. Peng, *J. Chem. Soc., Dalton Trans.*, 1992, 2675; (*j*) W. J. Vining, G. A. Neyhart, S. Nielsen and B. P. Sullivan, *Inorg. Chem.*, 1993, **32**, 4214.
5 (*a*) M. Geissler, J. Kopf, B. Schubert, E. Weiss, W. Neugebauer and P. Von R. Schleyer, *Angew. Chem., Int. Ed. Engl.*, 1987, **26**, 587; (*b*) J. A. Ladd and J. Parker, *J. Chem. Soc., Dalton Trans.*, 1972, 930.
6 D. D. Perrin and W. L. F. Armarego, *Purification of Laboratory Chemicals*, 3rd edn., Pergamon, Oxford, 1988.
7 J. N. Demas and G. A. Crosby, *J. Phys., Chem.*, 1971, **75**, 991.
8 J. M. Calvert, J. V. Caspar, R. A. Binstead, T. D. Westmoreland and T. J. Meyer, *J. Am. Chem. Soc.*, 1982, **104**, 6620.
9 R. R. Gagne, C. A. Koval and G. C. Lisensky, *Inorg. Chem.*, 1980, **19**, 2854.
10 J. Chatt, J. D. Garforth and G. A. Rowe, *J. Chem. Soc. A*, 1966, 1834.
11 (*a*) P. T. Beurskens, G. Admiraal, G. Beursken, W. P. Bosman, S. Garcia-Granda, R. O. Gould, J. M. M. Smits and C. Smykalla, PATTY & DIRDIF92: The DIRDIF program system, Technical Report of the Crystallography Laboratory, University of Nijmegen, 1992; (*b*) TEXSAN-TEXRAY Structure Analysis Package, Molecular Structure Corporation, Houston, TX, 1985.
12 A. B. P. Lever, *Inorganic Electronic Spectroscopy*, 2nd edn., Elsevier, Amsterdam, 1984, pp. 221–222.
13 J. A. Paradis, D. W. Wertz and H. H Thorp, *J. Am. Chem. Soc.*, 1993, **115**, 5308.
14 P. A. Shapley, R. M. Marshman, J. M. Shusta, Z. Gebeyehu and S. R. Wilson, *Inorg. Chem.*, 1994, **33**, 498.
15 R. Ballardini, G. Varani, M. T. Indelli, F. Scandola and V. Balzani, *J. Am. Chem. Soc.*, 1978, **100**, 7219; D. G. Nocera and H. B. Gray, *J. Am. Chem. Soc.*, 1981, **103**, 7349.
16 T. Ohno and S. Kato, *Bull. Chem. Soc. Jpn.*, 1984, **57**, 1528; T. Shida and W. H. Hamill, *J. Chem. Phys.*, 1966, **44**, 2369.

Received 23*rd October* 1995; *Paper* 5/06969F